

## EXPERIMENTALLY DETECTING KELVIN–HELMHOLTZ ROLLER STRUCTURES OVER RIBLETS

### Wagih Abu Rowin

Department of Mechanical Engineering  
University of Melbourne  
Parkville, Victoria 3010, Australia  
waburowin@unimelb.edu.au

### Rahul Deshpande

Department of Mechanical Engineering  
University of Melbourne  
Parkville, Victoria 3010, Australia  
rahul.deshpande@unimelb.edu.au

### Sicong Wang

Department of Mechanical Engineering  
University of Melbourne  
Parkville, Victoria 3010, Australia  
sicongw@student.unimelb.edu.au

### Melissa Kozul

Department of Mechanical Engineering  
University of Melbourne  
Parkville, Victoria 3010, Australia  
kozulm@unimelb.edu.au

### Richard Sandberg

Department of Mechanical Engineering  
University of Melbourne  
Parkville, Victoria 3010, Australia  
richard.sandberg@unimelb.edu.au

### Nicholas Hutchins

Department of Mechanical Engineering  
University of Melbourne  
Parkville, Victoria 3010, Australia  
nhu@unimelb.edu.au

## ABSTRACT

This study introduces a methodology to detect quasi-two-dimensional spanwise structures over riblets, known as Kelvin-Helmholtz (K–H) rollers, using conventional hot-wire anemometry. The methodology is founded on the characteristic features of K–H rollers, known for their short wavelength in the streamwise direction and elongated large wavelength in the spanwise direction. Previous numerical investigations have indicated that although these structures originate near the crests of riblets, their fluctuation effects can be detected within the valleys of the riblets. Based on this knowledge, two normal single hot-wires were deployed initially within the valleys of adjacent saw-tooth riblets and subsequently with a spanwise separation of five riblets. One of the wires was traversed in the wall-normal direction while the other remained stationary within a riblet valley to assess the extent of the rollers in this direction. A cross-correlation analysis is conducted on the signals acquired from the two wires in the spectral space. The analysis reveals a strong correlation between the two hot-wire signals placed one riblet apart along the span positioned below the riblet crest. The detected correlation is at a frequency higher than that associated with the characteristic near-wall cycle. This high-frequency correlation is hypothesised to be the spectral signature of the K–H rollers in the streamwise velocity fluctuations. These high-frequency signatures are also observed below the roughness crest when the wires are placed five riblets apart. These outcomes, which are consistent with the previous findings in the literature, demonstrate the efficacy of the methodology developed for detecting K–H rollers.

## INTRODUCTION

Riblets are flow aligned microgrooves that are well known for their drag reduction capabilities. The efficacy of riblets, measured by the reduction in drag compared to a smooth wall, depends on their viscous scaled size, assessed through the square root of the groove area, denoted as  $l_g = \sqrt{A_g}$  (Garcia-Mayoral & Jimenez, 2011b, 2012). Previous research has shown that drag reduction approaches a maximum value of approximately 10% when  $l_g^+ \approx 10$  (Garcia-Mayoral & Jimenez, 2011b). Here, superscript ‘+’ signifies normalisation by the friction velocity  $U_\tau$  and the kinematic viscosity  $\nu$ . However, as  $l_g^+$  continues to increase, riblets lose their drag-reducing ability and instead result in an increase in drag for  $l_g^+ \gtrsim 18$  (Garcia-Mayoral & Jimenez, 2011b, 2012). One widely discussed hypothesis attributes the drag increase over riblets to the formation of elongated quasi-two-dimensional spanwise structures, known as Kelvin-Helmholtz (K–H) like rollers, near the riblet crest (Garcia-Mayoral & Jimenez, 2011b). More recent studies have also linked K–H rollers to the breakdown of Reynolds analogy, where the enhancement in heat transfer surpasses the rise in frictional drag over blade riblets (Kuwata, 2022) and sawtooth riblets (Rouhi *et al.*, 2022). Simulation-based investigations have suggested the presence of K–H rollers by analysing the fluctuating wall-normal velocity signatures in the buffer layer, just above the plane of the riblet tips. These K–H rollers exhibit a quasi-periodic streamwise spacing. However, the exact mechanisms by which these features contribute to increased drag remain unclear, with some riblet geometries exhibiting very weak K–H contributions even within the drag increasing regime (Endrikat *et al.*, 2021).

To the best of the author’s knowledge, previous investigations that characterized the K–H rollers over riblets have

1. Adjustable roof
2. Traverse mechanism at measurement location at  $x = 3800$  mm
3. Working section with dimensions of  $L \times H \times W = 6700 \times 380 \times 940$  mm<sup>2</sup>
4. Contraction
5. Honeycomb and meshes
6. Diffuser
7. Centrifugal fan

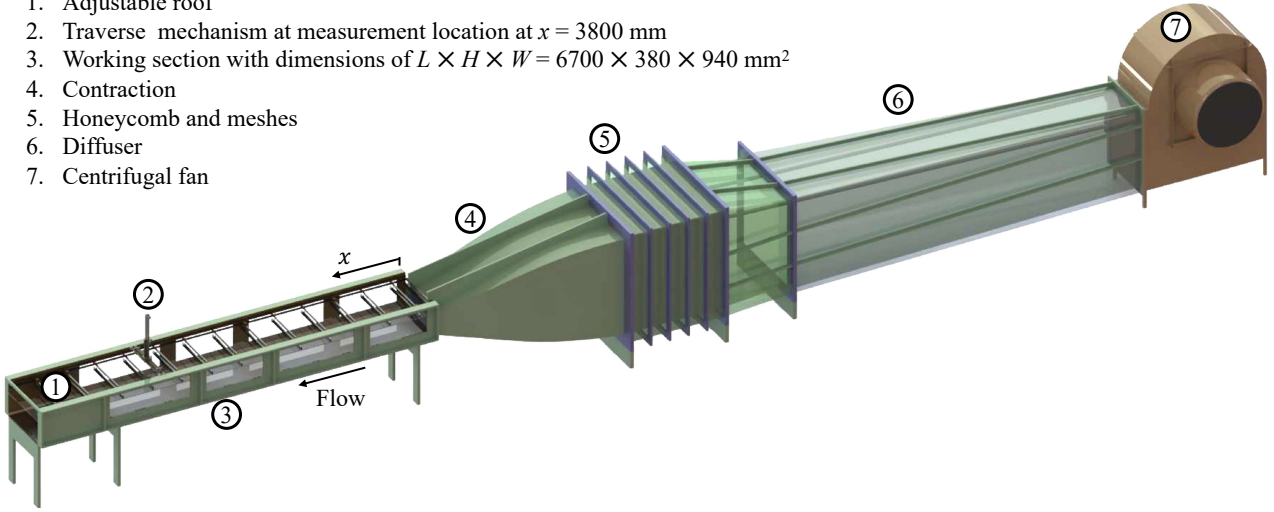


Figure 1. Schematic showing the wind tunnel facility including the working section and traverse located at the measurement location.

primarily relied on simulations (García-Mayoral & Jiménez, 2011a; Endrikat *et al.*, 2021; Kuwata, 2022; Rouhi *et al.*, 2022). These simulations have suggested that detecting K-H rollers could involve analysing two-dimensional spectra or co-spectra of Reynolds shear stress in the vicinity or within the valleys of the riblets. However, experimental verification of these findings is challenging due to the small size of the riblets and limitations in measurement techniques. For instance, capturing two-dimensional spectra near riblet crests requires techniques such as particle image velocimetry in the streamwise/wall-normal plane, multi-component laser doppler velocimetry, or multi-wire hot-wire anemometry, all of which are prone to spatial resolution issues and other systematic errors when applied near textured geometries. These challenges could potentially be overcome if K-H rollers could be detected solely through their streamwise velocity signatures, which can be conveniently obtained using a suitably miniaturised single normal hot-wire sensor.

This study experimentally examines the presence of K-H rollers over sawtooth riblets through a novel methodology based on streamwise velocity. The riblets studied here feature a 30° tip angle and peak-to-peak spanwise spacing of  $s = 2$  mm. The experiments are conducted at a wind tunnel facility operated at a freestream velocity  $U_\infty = 5$  m s<sup>-2</sup> resulting in a viscous scaled groove area of approximately  $l_g^+ \approx 26$ . This particular riblet size was chosen based on the detection of K-H rollers in simulations conducted by Endrikat *et al.* (2021) over riblets of comparable shape and viscous scaled dimensions.

## EXPERIMENTAL SETUP

Experiments are performed in an open return wind-tunnel facility with working section dimensions of  $L \times H \times W = 6700 \times 380 \times 940$  mm<sup>2</sup> in the streamwise  $x$ -, wall-normal  $z$ - and spanwise  $y$ -directions, as shown in the schematic in Figure 1. Here  $x$  is the streamwise distance from a turbulence trip at the inlet to the working section. Full details about this facility are available in AbuRowin *et al.* (In-press). A  $5.7 \times 0.7$  m<sup>2</sup> area ( $x \times z$ ) of the tunnel floor is covered with a 30° sawtooth riblet surface. The riblet peak-to-peak spanwise distance is  $s = 2$  mm and height  $h_r = 3.3$  mm. The tunnel is operated at a constant freestream

velocity of  $U_\infty = 5$  ms<sup>-1</sup>. The reason for selecting this velocity is to ensure viscous scaled riblet spacing  $s^+ = sU_\tau/\nu = 26.7$ , which is comparable to the size of sawtooth riblets simulated by Endrikat *et al.* (2021), which demonstrated preservation of the K-H rollers. Throughout this work the uppercase velocity  $U$  denotes time-averaged velocity, while lowercase  $u$  denotes velocity fluctuations.

## METHODOLOGY

The experimental technique developed in this study is based on the distinctive characteristics of K-H rollers, which are known for their short wavelength in the streamwise direction and elongated large wavelength in the spanwise direction. Based on this understanding, we utilised two hot-wire probes positioned within the valleys of spanwise adjacent riblets and traversing in the wall-normal direction, to detect spanwise correlations at the relative low streamwise wavelengths associated with the K-H rollers. Given the small size of the riblets, with a peak spacing of  $s = 2$  mm, we modified two Dantec boundary layer type probes (55P15) to enable the sensor to descend the mid-height of the riblets. The modified probes featured a prong-to-prong spacing of 1.0 mm. For sensor preparation, a Wollaston wire with a Pt-core diameter of 2.5 μm was utilised, with an exposed wire length of approximately 0.5 mm enabled through etching using nitric acid. The length of the stubs on either side of the Pt sensor was maintained at approximately 0.1 mm to prevent conduction losses from the prongs. The probes were operated in constant temperature mode using a custom-designed Melbourne University constant temperature anemometer (MUCTA), with an overheat ratio of 1.8. Probe calibration was conducted in the freestream of the wind tunnel both before and after each velocity profile measurement. All measurements were taken at a streamwise location of  $x = 3.8$  m, as indicated by ② in Figure 1.

To validate the shortened sensor, measurements were initially conducted over a smooth wall at  $U_\infty = 5$  m s<sup>-1</sup>. The viscous scaled mean streamwise velocity ( $U^+ = U/U_\tau$ ) over the smooth wall is shown in Figure 2. The law-of-the-wall ( $U^+ = z^+$ ) and the log-law ( $U^+ = \kappa^{-1} \log z^+ + A$ , with  $\kappa = 0.384$  and  $A = 4.17$ ) are included for comparison. Additionally, the mean velocity profile from simulations over a smooth wall of

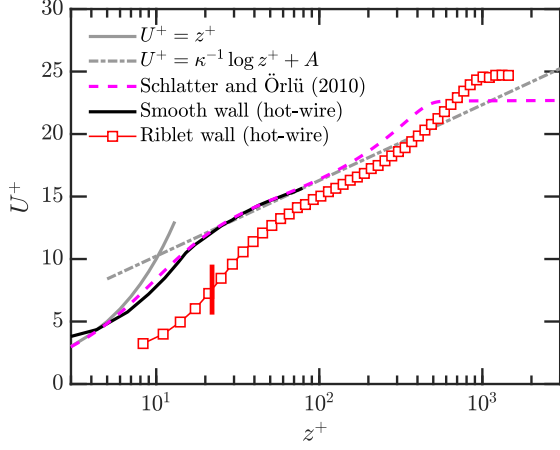


Figure 2. Mean viscous scaled streamwise velocity  $U^+$  as function of the viscous scaled wall-normal distance  $z^+$ . The short vertical red line indicates height of the riblet crest.

Schlatter & Örlü (2010) at  $Re_\tau \approx 670$  is provided for reference. The friction velocity  $U_\tau = 0.177$  is estimated for the experimental data using a Clauser fit. The overlap observed between the velocity profile measured by the modified probe, within a limited wall-normal height, with the log-law, as well as the profile from the simulation, confirms the validity of the modified probe.

After validating the modified probe, measurements were conducted over the riblet wall at  $U_\infty = 5 \text{ m s}^{-1}$ . The origin  $z = 0$  was set at the mid-height of the riblet ( $h_r/2$ ). Careful traversing of the modified wire was performed within the valley (as shown in Figure 3), approaching a lowest point of  $z = 500 \mu\text{m}$  above the riblet mid-height, measured with a camera microscope. The friction velocity over the riblets at the current  $U_\infty$  was determined to be  $U_\tau = 0.200 \text{ m/s}$  using the Clauser method. It should be noted that selecting the virtual origin at the riblet mid-height may have an effect on the estimated  $U_\tau$ , but any associated uncertainty should not affect the developed technique for detecting K–H rollers. At this  $U_\tau$ , the viscous scaled riblet size is  $s^+ = 26.7$  and  $l_g^+ = 25.7$ . Figure 2 illustrates that  $U^+$  over the riblets is lower than that over the smooth wall, suggesting that the current riblet size falls within the drag-increasing regime, thereby indicating the possibility of K–H roller existence, as previously demonstrated by Endrikat *et al.* (2021).

Having confirmed that the riblets at the current viscous scale are operating in the drag increasing regime, we placed two normal wires within the valleys of the riblets at the same streamwise ( $x$ ) location and finite spanwise separation, referred to as  $\Delta y$ . The rationale of deploying the wires within the valleys, instead of placing them above the crest of the riblets, is based on the investigation of Sharma & García-Mayoral (2020), where they reported that the influence of K–H rollers is easily observed deep into the valleys, despite their origin at the crest of the riblets. We also expect relatively less turbulence activity in the riblet valleys, compared to that above the riblet tips, thereby facilitating detection of the rollers in the spectral domain. To understand the wall-normal extent of these structures, we kept one of the wires stationary within the valley of the riblets, while the other is traversed across the wall-normal direction. Initially, since these structures are be-

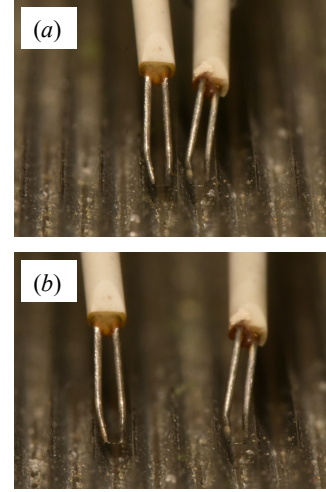


Figure 3. Pictures of the two wires deployed within the valleys of the riblets when the spanwise spacing between the wires is (a)  $\Delta y/s = 1$  and (b)  $\Delta y/s = 3$ .

lieved to extend to at least one riblet spacing due to the inherent nature of the rollers (García-Mayoral & Jiménez, 2011a; García-Mayoral & Jimenez, 2012), we placed the two wires within adjacent riblets with  $\Delta y \equiv s = 2 \text{ mm}$  (i.e.  $\Delta y/s = 1$ ) as shown in Figure 3(a). At this spanwise separation, various turbulent structures are expected to be detected by the two wires including the K–H rollers. For this reason, we extended the spanwise distance between the two wires gradually, as shown in Figure 3(b), at intervals of  $s$ , until we reached  $\Delta y/s = 5$  (i.e.  $\Delta y^+ = 135$ ). At this spanwise separation, only the large structures (Deshpande *et al.*, 2021) and the K–H rollers are expected to be detected by the two wires.

We apply the well-established strategy of reconstructing the two-point correlations in the spectral domain (Del Alamo *et al.*, 2004; Bailey *et al.*, 2008; Baars *et al.*, 2017; Deshpande *et al.*, 2021) of the signals acquired by the two wires. The cospectra  $\phi$  of streamwise velocity fluctuations is computed as

$$\phi_{uu_r}(z, z_r, \Delta y; T) = \tilde{u}(z, y, T) \tilde{u}^*(z_r, y_r; T), \quad (1)$$

where  $\tilde{u}(z, y, T)$  indicates the Fourier transform of  $u(z, \Delta y)$  in  $T$  time. The asterisk ‘\*’ denotes the complex conjugate and the superscript ‘r’ indicates the reference signal acquired by the stationary wire within the valley of the riblet.

### CO-SPECTRA OF STREAMWISE VELOCITY

Figure 4(a) depicts the normalised cospectra of streamwise velocity fluctuations  $k_x \phi_{uu_r}^+$  as a function of the viscous-scaled time scale  $T^+ = U_\tau^2 / f\nu$  of a fixed signal ( $u_r$ ) situated at the riblet mid-height, alongside another wall-normal traversing signal when the two wires are positioned in adjacent riblets with  $\Delta y/s = 1$ . Here,  $f$  represents frequency. A discernible positive correlation is evident between the two signals below the riblet crest, observed within the range of  $20 \lesssim T^+ \lesssim 100$  and peaking at  $T^+ \approx 50$ , as indicated by the black rectangle in Figure 4(a). It is expected to observe this positive correlation extending slightly above the riblet crests before rapidly diminishing, considering that K–H rollers are known to form above

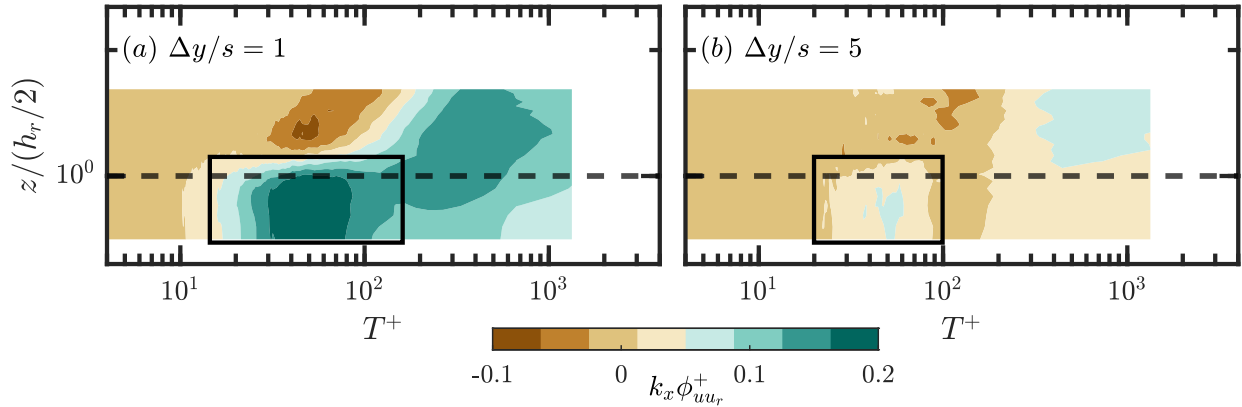


Figure 4. Normalised cospectra at  $U_\infty = 5 \text{ ms}^{-1}$  when (a)  $\Delta y/s = 1$  and (b)  $\Delta y/s = 5$ . The horizontal dashed black lines are at the riblet crest and the black rectangles are highlighting the positive correlation below the roughness crest.

the riblet peaks (García-Mayoral & Jiménez, 2012). The negative and positive correlations noted above the riblet crests in Figure 4(a), at  $T^+ \lesssim 100$  and  $T^+ \gtrsim 100$  respectively, are indicative of the hierarchy of turbulent scales over the riblet crest (Deshpande *et al.*, 2021).

To ascertain the efficacy of the developed method for identifying K–H rollers at larger spanwise separations between the wires, we plot in Figure 4(b) the  $k_x \phi_{uu_r}^+$  when  $\Delta y/s = 5$  (i.e.,  $\Delta y^+ \approx 135$ ). We only concentrate on  $\Delta y/s = 5$  for brevity, as it exemplifies the extreme case of the gathered data. A positive correlation emerges at  $T^+ \approx 1000$ , which can be expected given its association with large-scale structures (Baars *et al.*, 2017; Deshpande *et al.*, 2021). Interestingly, a positive correlation is also detected below the riblet crest at  $T^+ \approx 50$  in Figure 4(b), akin to the frequency observed when  $\Delta y/s = 1$  in Figure 4(a), presumably corresponding to the frequency of the K–H rollers. This observation confirms the experimental feasibility of the developed method in detecting the K–H rollers solely from the streamwise velocity signal.

## CONCLUSION

The experimental investigation presented in this study aims to introduce a novel technique for detecting Kelvin–Helmholtz (K–H) like rollers over riblets. Leveraging the characteristic features of these rollers, which exhibit a short wavelength in the streamwise direction and an elongated large wavelength in the spanwise direction, the method seeks to identify their presence within the valleys of riblets. Previous numerical simulations have suggested that while these structures originate near the crests of riblets, their signature can extend into the valleys. To explore this phenomenon, two normal single hot-wires were positioned within the valleys of adjacent saw-tooth riblets, with one wire traversing in the wall-normal direction while the other remained stationary. A cross-correlation analysis between the signals acquired from these wires was then employed to assess the presence of K–H rollers.

The results of the experimental investigation provided compelling evidence of the efficacy of the developed method in detecting K–H rollers. A strong correlation between the signals from the two wires at low streamwise wavelengths was observed below the riblet crest when placed one riblet apart in the spanwise direction. Ordinarily, in the smooth wall turbu-

lent boundary layer, correlations at this streamwise wavelength (corresponding to  $T^+ = 50$ ) would not be expected to persist over extended spanwise distances. The fact that this correlation persisted for the riblets even when the wires were positioned five riblets apart, provides strong evidence that we are detecting the K–H rollers. Notably, no correlation with other turbulence scales was found at this spanwise distance except the expected large scales, further underscoring the specificity of the developed technique for detecting K–H rollers.

## 1 ACKNOWLEDGEMENT

The authors appreciate the financial support of the Australian Research Council. W. Abu Rowin and R. Deshpande gratefully acknowledge financial support from the University of Melbourne through the Early Career Researcher grant and the Melbourne Postdoctoral Fellowship, respectively.

## REFERENCES

- Abu Rowin, W., Xia, Y., Wang, S. & Hutchins, N. In-press Accurately predicting turbulent heat transfer over rough walls: A review of measurement equipment and methods. *Exp. Fluids*.
- Baars, Woutijn J, Hutchins, Nicholas & Marusic, Ivan 2017 Self-similarity of wall-attached turbulence in boundary layers. *J. Fluid Mech.* **823**, R2.
- Bailey, Sean CC, Hultmark, Marcus, Smits, Alexander J & Schultz, Michael P 2008 Azimuthal structure of turbulence in high reynolds number pipe flow. *J. Fluid Mech.* **615**, 121–138.
- Del Alamo, Juan C, Jiménez, Javier, Zandonade, Paulo & Moser, Robert D 2004 Scaling of the energy spectra of turbulent channels. *J. Fluid Mech.* **500**, 135–144.
- Deshpande, R., de Silva, C., M., Lee, M., Monty, J. & Marusic, I. 2021 Data-driven enhancement of coherent structure-based models for predicting instantaneous wall turbulence. *Int. J. Heat Fluid Flow* **92**, 108879.
- Endrikat, S., Modesti, D., García-Mayoral, R., Hutchins, N. & Chung, D. 2021 Influence of riblet shapes on the occurrence of Kelvin–Helmholtz rollers. *J. Fluid Mech.* **913**.
- García-Mayoral, R. & Jiménez, J. 2011a Drag reduction by riblets. *Philos. T. R. Soc. A* **369** (1940), 1412–1427.

- García-Mayoral, R. & Jiménez, J. 2011b Hydrodynamic stability and breakdown of the viscous regime over riblets. *J. Fluid Mech.* **678**, 317–347.
- García-Mayoral, R. & Jiménez, J. 2012 Scaling of turbulent structures in riblet channels up to  $Re_\tau \approx 550$ . *Phys. Fluids* **24**, 105101.
- Kuwata, Y 2022 Dissimilar turbulent heat transfer enhancement by Kelvin–Helmholtz rollers over high-aspect-ratio longitudinal ribs. *J. Fluid Mech.* **952**, A21.
- Rouhi, A., Endrikat, S., Modesti, D., Sandberg, R., D., Oda, T., Tanimoto, K., Hutchins, N. & Chung, D. 2022 Riblet-generated flow mechanisms that lead to local breaking of reynolds analogy. *J. Fluid Mech.* **951**, A45.
- Schlatter, P & Örlü, R 2010 Assessment of direct numerical simulation data of turbulent boundary layers. *J. Fluid Mech.* **659**, 116.
- Sharma, A. & García-Mayoral, R. 2020 Turbulent flows over dense filament canopies. *J. Fluid Mech.* **888**.